Genotypic and Gene Expression Studies in Congenital Melanocytic Nevi: Insight into Initial Steps of Melanotumorigenesis

Barbara Dessars[1,7], Linda E. De Raeve[2,7], Renato Morandini[3], Anne Lefort[1], Hakim El Housni[4], Ghanem E. Ghanem[3], Benoît J. Van den Eynde[5], Wenbin Ma[5], Diane Roseeuw[2], Gilbert Vassart[1,4], Frédérick Libert[1,8] and Pierre Heimann[4,6,8]

Large congenital melanocytic nevi (CMNs) are said to have a higher propensity to malignant transformation compared with acquired nevi. Thus, they represent a good model for studying initial steps of melanotumorigenesis. We have performed genotypic (karyotype, fluorescence *in situ* hybridization, and mutational analyses) and differential expression studies on a large cohort of medium ($n=3$) and large ($n=24$) CMN. Chromosomal abnormalities were rare and single, a feature probably reflecting the benignity of these lesions. Mutational screening showed a high frequency of *NRAS* mutations in our series (19/27 cases, 70%), whereas *BRAF* mutations were less common (4/27 cases, 15%). Differential did not show significant alterations of cellular processes such as cell proliferation, cell migration/invasion, angiogenesis, apoptosis, and immune/inflammatory responses. However, significant downregulation of genes involved in pigmentation and upregulation of genes playing a role in DNA protection were observed. Lastly, our microarrays displayed upregulation of genes mediating chemoresistance in cancer. As alteration of pigmentation mechanisms can trigger oxidative damage, increased expression of genes involved in maintenance of DNA integrity might reflect the ability of nevocytic cells to self-protect against cellular stress. Furthermore, the observed alterations linked to chemoresistance might partially account for the well-known inefficacy of chemotherapy in malignant melanoma.

Journal of Investigative Dermatology (2009) **129,** 139–147; doi:10.1038/jid.2008.203; published online 17 July 2008

INTRODUCTION

Large congenital melanocytic nevi (CMNs), that is, larger than 20 cm in diameter, are found in about 1 out of 20,000 newborns (Hale *et al.*, 2005). Although there are still some controversies regarding the increased risk of malignant transformation in small (smaller than 1.5 cm in greatest diameter) and medium (from 1.5 to 19.9 cm in greatest diameter) CMNs, several studies have reported a 100- to 1,000-fold increased risk for the occurrence of melanoma in patients with large CMNs (Hale *et al.*, 2005). Although the majority of malignant melanoma occurs *de novo*, 20–30% arise from preexisting melanocytic nevi (Rivers, 2004). In the latter situation, one may assume that a multistep process involving sequential and cumulative genetic aberrations allows malignant melanoma to arise from a precursor melanocytic nevus. If genetic studies on metastatic malignant melanoma are numerous and extensive, molecular investigations on benign melanocytic lesions have been restricted to mutational and loss-of-heterozygosity analyses targeting the genes classically involved in tumorigenesis (Papp *et al.*, 2003; Pollock *et al.*, 2003). This is mainly due to the difficulty of performing large and diverse molecular studies on benign acquired nevi specimens that are entirely processed for morphological examination. Large CMNs contain a great number of melanocytic cells, allowing both histological examination and extensive genetic investigations. Therefore, large CMNs represent an excellent model to study and better understand the initial steps of melanocytic proliferation that sometimes precedes malignant transformation.

[1]*Inter-Disciplinary Research in Human and Molecular Biology Institute (IRIBHM), Faculty of Medicine, Université Libre de Bruxelles, Brussels, Belgium;* [2]*Department of Dermatology, Universitair Ziekenhuis Brussel, Vrije Universiteit Brussel, Brussels, Belgium;* [3]*Laboratoire d' Oncologie et de Chirurgie Expérimentale (LOCE), Bordet Institute, Brussels, Belgium;* [4]*Department of Medical Genetics, Erasme Hospital, Faculty of Medicine, Université Libre de Bruxelles, Brussels, Belgium;* [5]*Ludwig Institute for Cancer Research and Cellular Genetics Unit, Université Catholique de Louvain, Brussels, Belgium and* [6]*Department of Cytogenetics, Bordet Institute, Brussels, Belgium*

[7]*These two authors are shared first authors.*

[8]*These two authors are shared last authors.*

Correspondence: Dr Barbara Dessars, Inter-disciplinary Research in Human and Molecular Biology Institute (IRIBHM), Faculty of Medicine, Université Libre de Bruxelles, 808 Route de Lennik, Brussels 1070, Belgium. E-mail: bdessars@ulb.ac.be

Abbreviations: CMN, congenital melanocytic nevus; FISH, fluorescence in situ *hybridization; aRNA, antisense amplified RNA; HEEBO, human exonic evidence-based oligonucleotide; RT-PCR, reverse transcriptase-PCR; QRT-PCR, quantitative real-time RT-PCR; SD, standard deviation; SAM, significance analysis of microarray*

Received 20 July 2007; revised 13 May 2008; accepted 26 May 2008; published online 17 July 2008

Table 1. Karyotype, FISH *BRAF*, and mutational profile of the 27 studied CMN

Sample's reference	Large or Medium CMNs	Karyotype	FISH *BRAF*	Mutational screening *BRAF*	Mutational screening *NRAS*
NCG1	Large	N	NA	WT	Q61K
NCG2	Large	N	NA	WT	Q61K
NCG3	Large	N	NA	WT	Q61R
NCG4	Large	N	NA	WT	Q61R
NCG5	Large	N	NA	WT	Q61K
NCG6	Large	N	NA	WT	Q61K
NCG7	Large	N	NA	WT	Q61R
NCG8	Large	N	NA	WT	Q61K
NCG9	Large	N	NA	WT	Q61K
NCG10	Medium	N	NA	WT	WT
NCG11	Large	N	NA	WT	Q61K
NCG12	Large	N	NA	WT	Q61R
NCG13	Large	N	NA	WT	Q61K
NCG14	Large	N	NA	WT	Q61K
NCG15	Large	N	NA	WT	G13R
NCG16	Large	46,XY,add (6)(q21) [25]/46,XY [40]	NA	WT	Q61K
NCG17	Large	N	NA	WT	Q61K
NCG18	Medium	N	NA	WT	Q61K
NCG19	Large	N	NA	WT	Q61K
NCG20	Large	N	NA	WT	Q61K
NCG21	Large	N	NA	V600E	WT
NCG22	Large	N	NA	V600E	WT
NCG23	Medium	N	NA	V600E	WT
NCG24	Large	46,XY,t(2;7) (q24q33;q33q36) [40]	*BRAF* translocation	WT	WT
NCG25	Large	N	NA	WT	WT
NCG26	Large	N	NA	V600E	WT
NCG27	Large	46,XX,t(5;7)(q31;q34) [50]	*BRAF* translocation	WT	WT

CMN, congenital melanocytic nevi; FISH, fluorescence *in situ* hybridization; N, normal; NA, not amplified; WT, wild type.

RESULTS

Karyotype and FISH analyses

The karyotypes were normal in all but three CMNs. Two of them showed a chromosomal translocation involving the *BRAF* gene (chromosome 7q34), expected to drive activation of this oncogene (Stanton and Cooper, 1987; Heidecker *et al.*, 1990). Those cases have been described in an earlier paper (Dessars *et al.*, 2007). The third positive case displayed an add(6)(q21) chromosomal rearrangement that has not yet been molecularly investigated, but results in deletion of the whole 6q terminal region downstream to the 6q21 break point. In all cases with normal karyotype, fluorescence *in situ* hybridization (FISH) analysis did not demonstrate any *BRAF* chromosomal rearrangement or amplification. Results are detailed in Table 1.

Mutational screening of *BRAF/NRAS*

BRAF V600E mutations were found in 4/27 CMN (15%), and *NRAS* mutations in 19/27 CMN (70%). Among the four remaining cases negative for *BRAF* and *NRAS* mutations, two of them harbored a chromosomal translocation involving the *BRAF* oncogene. Results are detailed in Table 1.

Microarray experiments

Differential expression study of all 27 CMN cases using the "in-house made" slides. At first, we searched for common gene dysregulations among the whole CMN collection. Using a double selection ("significance analysis of microarray (SAM) one class" method (Tusher *et al.*, 2001), followed by further more stringent selection using a cutoff value of absolute normalized fold change >1.5 in any direction in $>75\%$ of

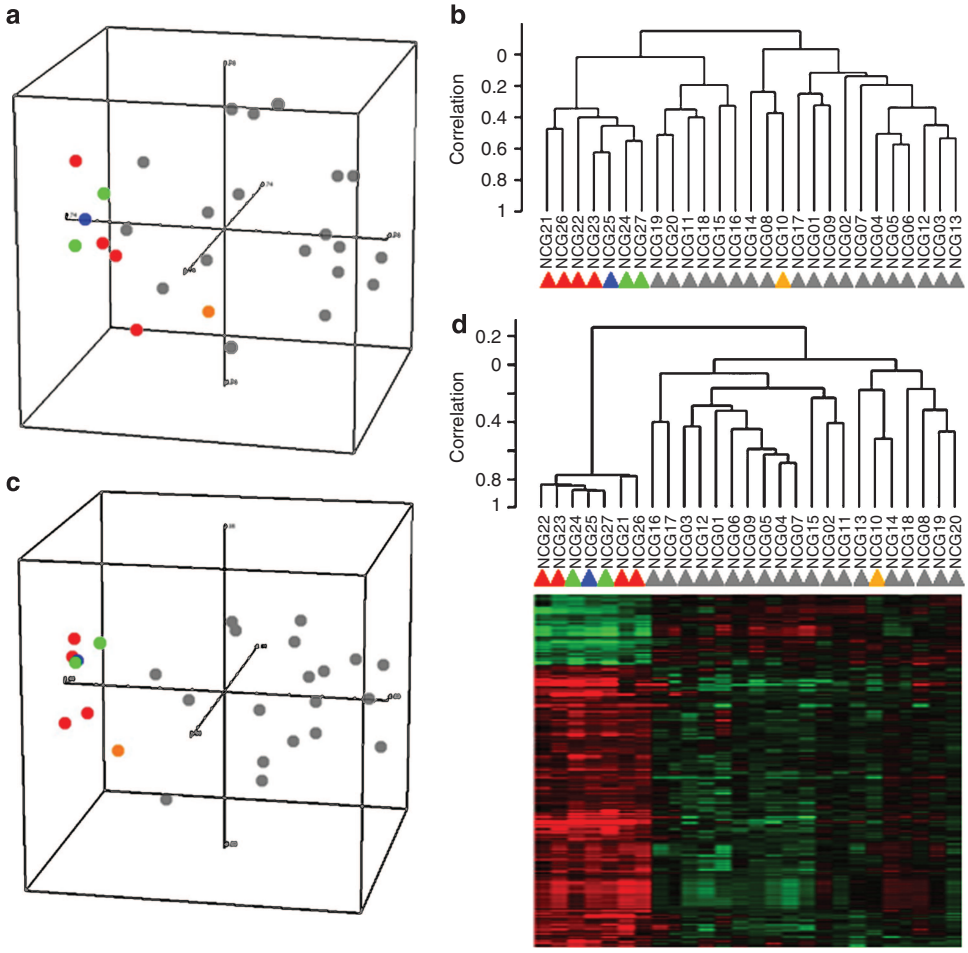

Figure 1. Multidimensional scaling analysis and hierarchical clustering of the 27 CMN studied. (**a**, **b**) Multidimensional scaling analysis and hierarchical dendrogram performed from the whole of genes and showing a close expression pattern for the six *BRAF*-activated (*BRAF*+) CMN group (four *BRAF*-mutated and two *BRAF*-translocated CMN). Analysis also revealed two other CMN cases clustering either with the *BRAF*+ group (NCG25) or with the *NRAS*+ group (NCG10). (**c**, **d**) Multidimensional scaling analysis and hierarchical clustering performed from the subset of genes selected by ''SAM 2 classes'' analysis and isolating more clearly the group composed of the six *BRAF*+ and NCG25 CMN from the remaining samples. The 4 *BRAF*-mutated CMN are represented by red-filled circles, the 2 *BRAF*-translocated CMN by green-filled circles, the 19 *NRAS*+ CMN by gray-filled circles, NCG25 by an orange-filled circle, and NCG10 by a blue-filled circle. Each filled circle represents an experiment derived from the mean of the triplicate log2 ratios of the ''in-house made'' microarrays. The distance between filled circles is proportional to the dissimilarity of expression profiles represented by those filled circles.

the samples, a list of 57 genes dysregulated in at least 21 out of the 27 CMNs investigated was consequently isolated, showing either up- (20) or downregulation (37) (Table S1c).

Secondly, we searched for CMN subgroups according to their respective gene expression profiles. The relationship between the CMN expression profiles was visualized by multidimensional scaling applied on all the genes. Multidimensional scaling reduces the high-dimensional gene space to a three-dimensional space while preserving between-samples distances (Figure 1a).

The multidimensional scaling revealed a close expression pattern for the six *BRAF*-activated (*BRAF*+) CMN group (hence, four *BRAF*-mutated and 2 *BRAF*-translocated CMNs) (Figure 1a). A hierarchical clustering confirmed this close expression pattern (Figure 1b). Analyses (multidimensional scaling and hierarchical clustering) also revealed two CMN cases clustering either with the *BRAF*+ group (NCG25) or with the *NRAS*+ group (NCG10), whereas sequencing of *BRAF* and *NRAS* exonic regions did not reveal any mutation in both cases (Table 1). *BRAF* and *NRAS* intronic regions were not sequenced due to their large length (around 190 kb in total). Moreover, no mutation was found in sequencing those two cases for all known *H*- and *K-RAS* mutations, including hot-spots codons 12, 13, and 61. A resampling analysis using all genes, by a bootstrapping approach, revealed that the node assembling the 6 *BRAF*+ and NCG25 samples was supported in 83% over the resampling trials, thus confirming the close pattern obtained with the multidimensional scaling and hierarchical clustering analyses (Saaed *et al.*, 2003—data not shown).

Significant changes in expression between the six *BRAF*+/NCG25 CMNs and the remaining cases were identified with SAM analysis, resulting in a list of 326 genes with a false discovery rate of less than 0.01% (Table S1e). The output table generated by ''SAM two unpaired classes'' analysis was compared with the leave-one-out cross-validation output

table, which contains a list of significant genes at $P<0.0001$ that are able to discriminate between the two classes (see Materials and Methods). It shows that all the SAM-selected genes were represented in leave-one-out cross-validation output file (data not shown).

A multidimensional scaling relative to this list of ''SAM-selected genes'' illustrated the existence of two subgroups of CMNs (Figure 1c). The subset of 326 genes was visualized among all the samples by hierarchical clustering using centered correlation and average linkage method (Figure 1d).

Results obtained from ''in-house made'' slides are provided in Table S1a–e.

Differential expression study using HEEBO slides of the four BRAF-mutated CMN cases. We have extended our genomic expression study to the four *BRAF*-mutated CMN cases by using human exonic evidence-based oligonucleotide (HEEBO) slides containing the whole genome.

Although a close expression pattern was observed for the six *BRAF*-activated CMN cases, chromosomal translocations involving *BRAF* have not been described as a genetic mechanism involved in the development of malignant melanoma. Furthermore, it cannot be excluded that the partner genes of *BRAF* involved in both translocations have any impact (even slight) on gene expression driven by *BRAF* activation itself. Thus, we have decided to limit this further study to the four cases harboring a single *BRAF* mutation. Those can be reasonably considered as being the most reliable benign counterpart of *BRAF*-mutated malignant melanoma.

Using the double selection described in the Materials and Methods section, 560 known genes commonly dysregulated were found (Table S2b). No obvious trend toward activation or inhibition of biological processes, such as cell proliferation, cell migration and invasion, angiogenesis, apoptosis, and immune and inflammatory responses, was observed. On the other hand, microarray analysis disclosed an expression profile associated with activation of cellular metabolism, activation of DNA repair mechanisms, reduction of melanin synthesis/distribution, as well as increased expression of genes leading to chemoresistance (Table S3). Results obtained from HEEBO slides are given in Table S2a, b.

Quantitative Real-Time RT-PCR

Quantitative real-time RT-PCR (QRT-PCR) was performed to validate microarray results from the HEEBO slides and was limited to 8 genes showing significant up- (*TIMP3*, *GAPDH*, *TFRC*, and *CCND1*) or downregulation (*ARL4C*, *ETS1*, *PMP22*, and *TACC1*) in the four *BRAF*-mutated samples. To validate our microarrays data by QRT-PCR, two control genes, *SDHA* and *TTC1*, were selected using geNorm program (http://medgen.ugent.be/genorm/; Vandesompele *et al.*, 2002). In seven out of eight tested genes (*ARL4C*, *ETS1*, *PMP22*, *TACC1*, *TFRC*, *TIMP3*, and *GAPDH*), statistic analysis of QRT-PCR results confirmed, in all samples, the significant gene dysregulations obtained by microarray analysis. For the remaining gene (*CCND1*), statistical significance was not reached in the four samples. In our series, we obtain a global concordance of $>90\%$, comparable with other studies (Pavey *et al.*, 2004). The data of the QRT-PCR are shown in comparison with the array data in Table S4.

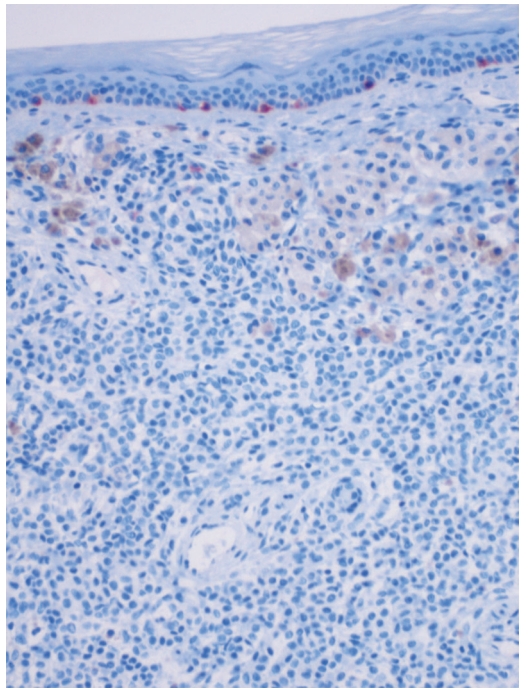

Figure 2. TYRP-1 immunohistochemical expression. NCG23 showing absence or very weak TYRP-1 expression of the intradermal nevic cells contrasting with strong positivity of normal epidermal melanocytes. TYRP-1 immunohistochemical features of the three other *BRAF*-mutated cases as well as of foreskin normal melanocytes are illustrated in the Figure S1.

Immunohistochemical studies targeting TYRP-1 protein

Among several antibodies tested (TYRP1, DCT, osteopontin, ALDH1A1, HSP90), TYRP-1 was the only one giving reliable results on positive tissue controls. Immunohistochemical study limited to this antibody demonstrated no or weak expression of the TYRP-1 protein in our *BRAF*-mutated CMNs compared with the intense positivity in the normal melanocytic counterpart (Figure 2 and Figure S1). Those results thus confirmed our microarray results for this protein.

DISCUSSION

Our study provides broad karyotypic, mutational, and differential expression data on a large series of medium and large CMN.

Rarity of karyotypic abnormalities in CMN

Karyotypic abnormalities were rare and single, including a chromosomal translocation involving the *BRAF* gene in two cases already published (Dessars *et al.*, 2007) and an add(6)(q21) resulting in deletion of a great part of chromosome 6q in a third case. In the context of multistep melanotumorigenesis, these karyotypes, either normal or

displaying single chromosomal aberrations, are in contrast with complex karyotypes seen in melanomas and probably reflect the benign character of these lesions. Few cytogenetic investigations on CMNs have been reported in the literature (Padilla *et al.*, 1988; Mancianti *et al.*, 1990; Heimann *et al.*, 1993). An earlier study used comparative genomic hybridization to analyze chromosomal aberrations in different types of large CMNs (Bastian *et al.*, 2002) and found neither chromosomal amplification nor deletion among their CMN cases without foci of cellular atypia.

Deletion of the long arm of chromosome 6 is observed in several types of malignant tumors, including malignant melanoma (http://atlasgeneticsoncology.org/), where it represents one of the most frequent karyotypic aberrations (Ozisik *et al.*, 1994; Bastian *et al.*, 1998). However, it has never been described in benign acquired as well as congenital nevi (Healy *et al.*, 1996; Bastian *et al.*, 2002; Casorzo *et al.*, 2005) apart from a single loss-of-heterozygosity study performed on paraffin-embedded benign nevi (Maitra *et al.*, 2002). The 6q chromosome is supposed to contain putative tumor suppressor genes not identified yet, although the *AIM1* (absent in melanoma 1) gene has been proposed as candidate (Ray *et al.*, 1996). Of note, this case also harbors an *NRAS* oncogene mutation (Table 1), which would be thus associated with a putative tumor suppressor gene deletion. Up till now and after a follow-up of 6 years, the patient has not developed any melanoma. Nevertheless, this patient could be at higher risk of malignant transformation.

NRAS mutations are more frequent than BRAF mutations in large CMN

A high incidence of *NRAS* mutations was observed among our large CMN cases (18/24), unlike small congenital and acquired nevi where *BRAF* mutations are more frequent (Pollock *et al.*, 2003; Papp *et al.*, 2005; Ichii-Nakato *et al.*, 2006). This observation could support the Ichii–Nakato's hypothesis (Ichii-Nakato *et al.*, 2006), suggesting that *NRAS* mutations exert stronger growth signals, resulting in larger nevi than those linked to *BRAF* mutations.

Among the four cases negative for *BRAF* or *NRAS* mutation, two of them presented a chromosomal translocation involving *BRAF*. Of note, Bauer *et al.* also described 6 out of 32 studied cases without any mutation (Bauer *et al.*, 2007). It might be interesting to perform karyotyping or *BRAF* FISH analyses on their negative cases to detect putative chromosomal translocation involving *BRAF*.

The link between *BRAF* mutation and UV exposure is complex. Indeed, this mutation is frequently found in melanomas arising on sites subject to intermittent acute sun exposure, but its occurrence is surprisingly rare in melanomas developing on chronically sun-exposed skin areas, being similar to the one observed in completely sun-protected mucosa (Maldonado *et al.*, 2003). However, this link could be supported by the low frequency of *BRAF* mutation obtained among our CMN series. Regarding *NRAS* mutations, which are more frequently found in melanomas on sun-exposed skin (Jiveskog *et al.*, 1998), the high frequency of such mutation in our CMN series demonstrates that UV exposure is not necessarily required to generate *NRAS* mutations in melanocytes.

Comparison of CMN with normal melanocyte transcriptome revealed an upregulation of osteopontin in tumoral nevocytic cells

We have performed microarray investigation to compare mRNA expression profiles between CMN and normal melanocytes. To the best of our knowledge, there is only one differential expression study performed on three large CMN (Dasu *et al.*, 2004), where the authors compared CMN transcriptome with normal control represented by fresh peritumoral skin tissue. We believe that their results are biased, as the skin is mainly composed of keratinocytes and contains few melanocytes. To study specific gene expression alterations encountered in melanocytic tumorigenesis, we thus aimed to compare pure nevocytic cells with their normal cellular counterpart, hence antisense amplified RNA (aRNA) obtained from 13 pooled human foreskins RNA. We are aware that the use of a pool of normal melanocytic aRNA makes assessment of intersample variation impossible, and that the subsequent data obtained become acutely susceptible to outlier samples. Furthermore, using a single pool for ''normal'' sample class makes it impossible to estimate variances between ''normal'' and ''nevocytic'' samples classes. These caveats could be obviously avoided by comparing separately each CMN with each normal melanocytic aRNA, but this approach would represent a huge financial and technical task.

In both ''in-house made'' and HEEBO slides, the differences in expression between tumoral and normal cells were generally weak. These weak dysregulations could reflect the benign nature of the tumors tested in which some autoregulation would be maintained. On the other hand, by upregulating growth regulatory cascades in melanocytes, the use of serum and growth factors required for cell cultures could partially mask the gene dysregulation caused by the oncogenic mutations. However, it was not possible to avoid this potential bias, as cellular culture from foreskin samples was an absolute prerequisite to get pure melanocytic samples. Indeed, it has been demonstrated that more than 10% of contaminating nontarget cells in a sample can lead to spurious identification of dysregulated genes (de Ridder *et al.*, 2005).

Our microarray analysis performed on ''in-house made'' slides showed 57 genes commonly dysregulated (Table S1c) in at least 21 of 27 CMN, a number surprisingly small, considering that most samples had an activating mutation or rearrangement involving *BRAF* or *NRAS*, two key genes in the sensitive *MAPK* pathway. Among the 20 upregulated genes, we pointed the *osteopontin* (*secreted phosphoprotein 1*). Osteopontin is a secreted extracellular matrix glycophosphoprotein involved in malignant cell attachment and invasion. In epithelial cancers such as breast cancer, high osteopontin expression is associated with early metastasis (El-Tanani *et al.*, 2006). *In vitro* studies showed that activated *RAS* oncogene leads to constitutive activation of the *Raf/MEK/ERK* signal transduction pathway, which in turn induces increased transcription of osteopontin (El-Tanani *et al.*, 2006).

Osteopontin upregulation is thus not surprising in our cases where *NRAS* and *BRAF* mutations are very frequent.

Expression profiles obtained with "in-house made" slides reveal two different CMN groups

A common expression profile (composed of 326 transcripts) among the six *BRAF*+ and the NCG25 samples was observed, discriminating them from the other 20 samples (19 *NRAS*+ and NCG10 samples) (Table S1e). Although the molecular alteration involving the *BRAF* gene is not the same (point mutation *versus* chromosomal translocation) among our six *BRAF*+ samples, their close expression pattern is not intriguing, as these gene abnormalities both lead to *BRAF* activation. It has been well demonstrated that the loss of the *BRAF* auto-inhibitory regulatory domain, as observed in our two *BRAF*-translocated CMN, induces a *BRAF* constitutive activation as with *BRAF* point mutations (Stanton and Cooper, 1987; Heidecker *et al.*, 1990). Nevertheless, as no evidence of *BRAF* involvement was documented in NCG25, it cannot be stated that *BRAF* activation is the driver of its transcription profile.

The different profile observed between the six *BRAF*+ and *NRAS*+ samples is a rather surprising result, as these two genes are components of the same pathway. A recent microarray study of 61 melanoma cell lines has also revealed a profile specific to *BRAF* mutant samples, isolating them from *NRAS* mutant cases (Pavey *et al.*, 2004). As all cell lines used were grown in the presence of serum, the authors suggested that the genes discriminating *BRAF* and *NRAS* mutant cells are those that are independent of *MAPK* pathway activation, a cellular pathway that is supposed to be constitutively activated in every cell line cultured with serum. This notion should imply that some of the genes involved in the *BRAF* mutant expression profile may not be necessarily direct targets of transcription factor that are ultimately activated by the *MAPK* pathway (Pavey *et al.*, 2004). We suggest that the culture conditions may not be sufficient to cause activation of the *MAP*K pathway at the same level as that triggered by *BRAF*-activating mutation. On the other hand, *NRAS* activates also the *PI3K* pathway, which could either amplify or reduce the activating effects of the *MAPK* pathway, depending on cell environment and gene involved.

Whole genomic expression profile (HEEBO slides) of the four BRAF-mutated cases revealed dysregulation in pigmentation, DNA damage repair, and chemoresistance mechanisms

Although we are aware of the small size of our *BRAF*-mutated series (four cases), we wanted to focus on the complete genomic expression linked to a mutation harbored by the majority of benign acquired nevi and malignant melanoma cases. The expression profile observed in these benign *BRAF*-mutated cases is supposed to be directly linked to the mutation itself, and not yet modulated by additional genetic abnormalities arising in the course of malignant melanoma.

No clear direction toward activation or inhibition of cellular processes such as cell proliferation, cell migration and invasion, angiogenesis, apoptosis, and immune and inflammatory responses was obtained (Table S3). However, a significant decreased expression of genes involved in melanin synthesis (*TYRP-1*, *DCT*, and *ATP7A*) as well as in melanosome maturation/trafficking and pigment distribution (*BBS5*, *HPS1*, *MYO5A*, *OSTM1*, and *RAB32*) was observed (Tables S2b and S3). Among those genes, *TYRP-1* and *DCT* are well-known upregulated targets of the *MITF* gene, one of the key actors in melanocytic proliferation, survival, and differentiation (Vance and Goding, 2004; Levy *et al.*, 2006). Their downregulation might imply reduced *MITF* activity, although a significant decrease in *MITF* mRNA expression was not observed in all cases (see Table S2a). Nevertheless, reduced *MITF* activity could occur through post-transcriptional regulation. In melanogenesis, two types of melanins are synthesized from dopaquinone: eumelanin and pheomelanin. *TYRP-1* and *DCT* are two key enzymes in the eumelanin pathway. A downregulation of both genes will lead to decreased eumelanin production, with subsequent increase in the proportion of intracellular pheomelanin. Pheomelanin has the tendency to generate, as by-products, hydrogen peroxides, superoxides, and hydroxyl radicals, all known triggers of oxidative stress, which in turn can induce DNA damage and subsequent genomic instability (Lin and Fisher, 2007). Of note, and with respect to DNA damage, our microarray study revealed upregulation of several genes involved in DNA protection (*MGST1*, *DDIT4*, *MT1A*, *MT1F*, *MT1G*, *MT1X*, *MT2A*, *PLK3*, *RND3*, *SMG1*, *STC1*) (Tables S2b and S3). Among these genes, the different metallothioneins cited, *RND3* as well as *MGST1* genes, are implicated in cellular protection from oxidative stress. *STC1* and *RND3* genes are upregulated by *BRCA1* and *p53*, respectively, two genes with pivotal roles in genomic stability, as either caretaker or gatekeeper (Kinzler and Vogelstein, 1997).

The downregulation of genes favoring melanin synthesis is rather surprising in the context of heavily pigmented lesions such as CMN. However, this tumoral pigmentation could be the consequence of reduced melanosome intracellular trafficking and extracellular melanin distribution due to downregulation of genes involved in such processes (see above), resulting in subsequent cytoplasmic pigment retention.

Interestingly, our microarray study demonstrated *HSP90* upregulation in mutated *BRAF* CMN (Tables S2b and S3). Of note, *HSP90* chaperone is required for stability of the *BRAF*V600E mutant, which is degraded in response to *HSP90* inhibitors (Grbovic *et al.*, 2006). This supports the potential utility of *HSP90* inhibitors (17-demethoxygeldanamycin), or immunotherapy targeting *HSP90*, in the treatment of melanoma with mutated *BRAF* (Neckers and Neckers, 2002; Becker *et al.*, 2004; Sharp and Workman, 2006).

Finally, a last interesting trend in our *BRAF*+ CMN cases is the upregulation of several genes mediating chemoresistance in many cancers (*ALDH1A1*, *BIRC7*, *CLU*, *GBP*, *MGST1*, and *TNFRSF12A*) (Tables S2b and S3). Although these features are more likely to have no impact on benign melanocytic lesions, they could partially account for the well-known inefficacy of chemotherapy in malignant melanoma.

In summary, we have performed genotypic and differential gene expression studies on the largest series of large and medium CMNs published to date. Unlike malignant melanoma, CMNs disclose rare and single chromosomal abnormalities, probably reflecting the benign nature of these lesions in the context of melanocytic neoplasia. Additional karyotypic aberrations are most likely needed for malignant transformation. According to the literature, the frequency of *NRAS* mutations is higher in medium CMNs than in small CMNs and acquired nevi (Pollock *et al.*, 2003; Papp *et al.*, 2005; Ichii-Nakato *et al.*, 2006). We observed that this frequency is even higher in our series of large CMNs. The medium and large CMNs could thus be considered as molecularly distinguishable from the small congenital and acquired nevi where *BRAF* mutations are predominant. Lastly, our differential expression study did not show significant alterations of the most common cellular processes such as cell proliferation, cell migration and invasion, angiogenesis, apoptosis, and immune and inflammatory responses. This point may reflect the benign stage of the lesions studied where activation of cellular behavior such as proliferation is still counterbalanced by inverse regulations, preventing therefore significant alterations that could compromise cellular steady state. Nevertheless, gene dysregulations emerged, particularly in pigmentation and DNA damage repair mechanisms, for which the biological significance still needs to be clarified.

MATERIALS AND METHODS

Patients

Materials from 3 medium and 24 large CMN were obtained from children treated by either curettage or excision. At diagnosis, none of them presented melanoma degeneration or cellular proliferation-mimicking melanoma. The follow-up duration is 1–11 years, and until now, none of these patients developed a melanoma (De Raeve and Roseeuw, 2002). Informed consent from patients and agreement of the Ethical Committee were obtained. This study respected the Declaration of Helsinki Principles.

Cell culture

Cells from CMN samples as well as normal melanocytes from 13 different foreskins were isolated using a collagenase/dispase preparation (Morandini R., personal communication). Cell cultures and RNA extraction methodologies are detailed in the Supplementary Materials and Methods.

Karyotype analyses

Slides preparation and G-banding were carried out as described earlier (Heimann *et al.*, 1998). Karyotypes were expressed according to the International System for Human Cytogenetic Nomenclature (1995).

FISH study

Fluorescence *in situ* hybridization analyses were performed as described earlier (Heimann *et al.*, 1998), on metaphase and interphase cells from each nevus culture, using the BAC RP11-25N5 (supplied by the Archives Group at the Sanger Institute, Cambridge, UK) spanning the *BRAF* gene on 7q34. At least 50 interphase nuclei were counted for each case.

RT-PCR and sequencing

Exons 11 and 15 of the *BRAF* gene as well as the whole *NRAS* coding sequence were screened in all patients, with the use of specific forward and reverse primers (Supplementary Materials and Methods). All known *H-* and *K-RAS* mutations, including hot-spots codons 12, 13, and 61 (http://www.sanger.ac.uk/genetics/CGP/cosmic), as well as the whole coding region of *BRAF*, were screened in the two CMN without *NRAS* or *BRAF* mutation/rearrangement.

The PCR conditions are described in Supplementary Materials and Methods. PCR products were sequenced with the same sets of primers as PCR.

Microarray experiments

aRNA synthesis, labeling, and microarray hybridization. aRNA synthesis and labeling are detailed in Supplementary Materials and methods. All fluorescently labeled aRNA from the 27 nevi were hybridized onto ''in-house made'' slides containing 40,368 spots with 7,657 identified cDNA, each nevus being cohybridized and compared with a pool of melanocyte aRNA from the 13 different foreskins (normal control). The cDNA used for the slides were isolated from cDNA libraries of CP64-MEL melanoma cell line, normal melanocyte, leukocytes, and fetal brain (Invitrogen, Carlsbad, CA). All hybridizations onto ''in-house made'' slides were performed in triplicate (including one dye-swapped hybridization). Dye-labeled aRNAs from the four *BRAF*-mutated CMN were subsequently cohybridized with normal control (pool of 13 foreskins) on HEEBO arrays (Stanford Functional Genomics Facility, California) containing 44,544 70mer probes. Hybridizations onto HEEBO slides were replicated with dye swap.

Microarray data analysis. Slides were scanned using a Molecular Devices 4000B laser scanner and expression levels were quantified using GenePix Pro 6.1 image analysis software (Axon Instruments, CA). Image acquisitions were performed with automatic photomultiplier gains adjustment. Artifact-associated spots were eliminated by both visual and software-guided flags. The fluorescence values were imported into Acuity 4.0 software package (Molecular Devices, Union City, CA). A nonlinear Lowess (locally weighted scatter plot) normalization method applied to each individual block (print-tip option) was carried out using Acuity 4.0 software. The resulting data files were used for further data analysis. Data obtained from mean of the normalized log 2 ratio calculated for each triplicate were used for multidimensional scaling and hierarchical clustering.

Statistical methods. The ''SAM one class'' method with the default parameters (Tusher *et al.*, 2001) was used to identify genes differentially expressed among all the samples hybridized on ''in-house made'' slides, as well as the ones differentially expressed among the four *BRAF*-mutated samples hybridized on HEEBO slides (Tables S1b, c and S2b). As we wished to isolate genes obviously dysregulated from this first list of ''SAM one class''-selected genes, a second more stringent selection was done by using a cutoff of absolute normalized fold change >1.5 in any direction in $\geqslant 75\%$ of the samples ($\geqslant 21/27$ CMN samples in microarray analysis from ''in-house made'' slides, Tables S1b and c, or $\geqslant 3/4$ *BRAF*-mutated samples in microarray analysis from HEEBO slides, Table S2b).

Pearson-centered correlation coefficients of normalized log 2 ratio were used to quantify the similarity between the samples.

Relationships among expression profiles were visualized by performing hierarchical clustering using centered correlation and average linkage algorithm (Figure 1b). The corresponding multidimensional scaling analysis, which provides a graphical representation of the distances among samples without forcing the samples into specific clusters, was performed using BRB-Array Tools 3.5 software (Figure 1a). A resampling analysis using a bootstrapping approach was performed on the complete set of genes, to evaluate the reliability of a close pattern between the six *BRAF*+ and NCG25 samples (Saaed *et al.*, 2003). A subset of genes differentially expressed between the two classes of unpaired samples (the six *BRAF*+ samples and NCG25 *versus* the remaining samples including NCG10) was identified by using a multivariate permutation test, namely SAM method (Tusher *et al.*, 2001), to ensure that the number of false discoveries did not exceed 0.01%. The multidimensional scaling and hierarchical clustering were repeated with this subset of genes (Figures 1c and d). To validate the selected genes by ''SAM two unpaired classes'' analysis, a resampling method, the leave-one-out cross-validation-procedure (available in BRB-Array Tools 3.5 software), was applied on the same two unpaired classes of samples (Molinaro *et al.*, 2005). With leave-one-out cross-validation, the cross-validation process omits one sample at a time. For each sample omitted, the entire analysis is repeated from scratch, including the determination of genes that are univariately significant on the reduced training sample. From this gene list, a multivariate predictor is constructed and applied to the sample that was omitted for determining to which of the two classes the given sample belongs. Several multivariate classification methods were used, including the compound covariate predictor, diagonal linear discriminant analysis and the nearest neighbor predictor (Simon *et al.*, 2003). This is repeated, omitting all of the samples one at a time.

Quantitative Real-Time RT-PCR

To confirm the validity of the microarray experiments (HEEBO slides), eight unique transcripts (*ARL4C*, *ETS1*, *PMP22*, *TACC1*, *TFRC*, *TIMP3*, *GAPDH*, and *CCND1*) showing significant up- or downregulation in nevic samples relative to the ''normal pool'' were assessed by QRT-PCR (SYBR Green).

A validation performed on an unrelated sample would have been the ideal situation. The incidence of large CMN being around 1/20,000, its occurrence will be of 5–6 cases per year in Belgium, as more or less 116,000 births are recorded per year (http://www.one.be/rap/.%5Crap%5Caccomp_autour_naissance.html), among which only 15% of cases would harbor a *BRAF* mutation. In brief, only one *BRAF*-mutated large CMN is expected each year in our country. This explains the fact that validations were performed on the same sample set that was used for the expression study and will be repeated once additional samples will be available.

Two control genes, succinate dehydrogenase complex subunit A (*SDHA*) and tetratricopeptide repeat domain 1 (*TTC1*), were selected using geNorm program (http://medgen.ugent.be/genorm/) (Vandesompele *et al.*, 2002), and used for normalization of the QRT-PCR results from the eight up- or downregulated transcripts mentioned above, using qBase v1.3.4 free software (http://medgen.ugent.be/qBase/) (Hellemans *et al.*, 2007). Each test sample was run in triplicate for all tested genes.

The PCR conditions are described in Supplementary Materials and Methods. The expression of each candidate gene was calculated as the ratio of the normalized expression of that gene in nevic samples to those in ''normal pool''. Comparisons between CMN and normal samples were performed with the one-way analysis of variance and Dunnett Multiple Comparisons tests.

Immunohistochemical studies

Immunohistochemical studies were performed to confirm the most relevant microarray results but had to be limited to antibodies available on the market: TYRP-1 (Abcam, Cambridge, UK), DCT (Abcam, Cambridge, UK), osteopontin (Abcam; R&Dsystems, Minneapolis, MN; Santa Cruz, CA), ALDH1A1 (Abcam) and HSP90 (Abcam) proteins. At first, all these antibodies were tested on their respective positive tissue controls (melanoma for TYRP-1, DCT and osteopontin, liver for ALDH1A1, and vesical carcinoma for HSP90), and TYRP-1 was the only antibody giving reliable results. Immunohistochemical studies on our CMN cases were then limited to TYRP-1.

Immunohistochemical methodologies are detailed in Supplementary Materials and Methods.

CONFLICT OF INTEREST

The authors state no conflict of interest.

ACKNOWLEDGMENTS

This work was supported by the FNRS (Grant FNRS—Télévie), and by the CHC (Children Hope Challenge). Frédérick Libert is a research associate of the FNRS. We thank Michael Fero and the staff of the Stanford Functional Genomics Facility for supplying us with the human exonic evidence-based oligonucleotide (HEEBO) microarrays used for this study. We also thank Isabelle Borsu, Marie-Jeanne Gebski, Marie-Lydie Pelgrims, Chantal Debussher, Marie-Jeanne Simons, and Sandra Strollo for their excellent technical assistance, and Vincent Detours, Stephane Swillens, and Pierre Sidon for their precious advices.

SUPPLEMENTARY MATERIAL

Table S1a. Microarray data from ''in-house made'' slides.

Table S1b. Selection of genes showing a common dysregulation in at least 21 out of the 27 CMN analyzed.

Table S1c. Selection of genes showing a common dysregulation in at least 21 out of the 27 CMN analyzed, but after having suppressed all ''not identified'' and redundant spots.

Table S1d. Subset of genes differentially expressed between the two classes of unpaired samples (six *BRAF*+ samples and NCG25 *versus* the remaining samples including NCG10) identified by significance analysis of microarray (''SAM two unpaired classes'').

Table S1e. Subset of genes differentially expressed among the two classes of unpaired samples (six BRAF+ samples and NCG25 *versus* the remaining samples including NCG10) identified by significance analysis of microarray(''SAM two unpaired classes''), but after having suppressed all ''not identified'' and redundant spots.

Table S2a. Microarray data from HEEBO slides of the 4 *BRAF* mutated samples.

Table S2b. Selection of genes showing a common dysregulation in at least three out of the four *BRAF*V600E+ CMN analyzed.

Table S3. List of gene up- and downregulations leading to either activation or inhibition of the most significant cellular processes.

Table S4. Comparison between microarray and QRT-PCR data obtained for the four *BRAF*-mutated CMN cases and regarding eight significantly dysregulated genes.

Figure S1. TYRP-1 immunohistochemical expression.

Supplementary Materials and Methods. Supplementary Materials and Methods for cell culture; list of forward and reverse primers and respective PCR conditions used to perform PCR investigations and sequencing, as well as

quantitative real-time RT-PCR; supplementary Materials and Methods for microarrays experiments and supplementary Materials and Methods for immunohistochemical studies.

REFERENCES

Bastian BC, LeBoit PE, Hamm H, Brocker EB, Pinkel D (1998) Chromosomal gains and losses in primary cutaneous melanomas detected by comparative genomic hybridization. *Cancer Res* 58:2170–5

Bastian BC, Xiong J, Frieden IJ, Williams ML, Chou P, Busam K *et al.* (2002) Genetic changes in neoplasms arising in congenital melanocytic nevi: differences between nodular proliferations and melanomas. *Am J Pathol* 161:1163–9

Bauer J, Curtin JA, Pinkel D, Bastian BC (2007) Congenital melanocytic nevi frequently harbor NRAS mutations but no BRAF mutations. *J Invest Dermatol* 127:179–82

Becker B, Multhoff G, Farkas B, Wild PJ, Landthaler M, Stolz W *et al.* (2004) Induction of Hsp90 protein expression in malignant melanomas and melanoma metastases. *Exp Dermatol* 13:27–32

Casorzo L, Luzzi C, Nardacchione A, Picciotto F, Pisacane A, Risio M (2005) Fluorescence *in situ* hybridization (FISH) evaluation of chromosomes 6, 7, 9 and 10 throughout human melanocytic tumorigenesis. *Melanoma Res* 15:155–60

Dasu MR, Barrow RE, Hawkins HK, McCauley RL (2004) Gene expression profiles of giant hairy naevi. *J Clin Pathol* 57:849–55

De Raeve LE, Roseeuw DI (2002) Curettage of giant congenital melanocytic nevi in neonates: a decade later. *Arch Dermatol* 138:943–7

de Ridder D, van der Linden CE, Schonewille T, Dik WA, Reinders MJ, van Dongen JJ *et al.* (2005) Purity for clarity: the need for purification of tumor cells in DNA microarray studies. *Leukemia* 19:618–27

Dessars B, De Raeve LE, El Housni H, Debouck CJ, Sidon PJ, Morandini R *et al.* (2007) Chromosomal translocations as a mechanism of BRAF activation in two cases of large congenital melanocytic nevi. *J Invest Dermatol* 127:1468–70

El-Tanani MK, Campbell FC, Kurisetty V, Jin D, McCann M, Rudland PS (2006) The regulation and role of osteopontin in malignant transformation and cancer. *Cytokine Growth Factor Rev* 17:463–74

Grbovic OM, Basso AD, Sawai A, Ye Q, Friedlander P, Solit D *et al.* (2006) V600E B-Raf requires the Hsp90 chaperone for stability and is degraded in response to Hsp90 inhibitors. *Proc Natl Acad Sci USA* 103:57–62

Hale EK, Stein J, Ben Porat L, Panageas KS, Eichenbaum MS, Marghoob AA *et al.* (2005) Association of melanoma and neurocutaneous melanocytosis with large congenital melanocytic naevi—results from the NYU-LCMN registry. *Br J Dermatol* 152:512–7

Healy E, Belgaid CE, Takata M, Vahlquist A, Rehman I, Rigby H *et al.* (1996) Allelotypes of primary cutaneous melanoma and benign melanocytic nevi. *Cancer Res* 56:589–93

Heidecker G, Huleihel M, Cleveland JL, Kolch W, Beck TW, Lloyd P *et al.* (1990) Mutational activation of c-raf-1 and definition of the minimal transforming sequence. *Mol Cell Biol* 10:2503–12

Heimann P, Ogur G, De Busscher C, Morandini R, Libert A, Vamos E (1993) Chromosomal findings in cultured melanocytes from a giant congenital nevus. *Cancer Genet Cytogenet* 68:74–7

Heimann P, Devalck C, Debusscher C, Sariban E, Vamos E (1998) Alveolar soft-part sarcoma: further evidence by FISH for the involvement of chromosome band 17q25. *Genes Chromosomes Cancer* 23:194–7

Hellemans J, Mortier GR, De Paepe A, Speleman F, Vandesompele J (2007) qBase relative quantification framework and software for management and automated analysis of real-time quantitative PCR data. *Genome Biol* 8:R19

Ichii-Nakato N, Takata M, Takayanagi S, Takashima S, Lin J, Murata H *et al.* (2006) High frequency of BRAFV600E mutation in acquired nevi and small congenital nevi, but low frequency of mutation in medium-sized congenital nevi. *J Invest Dermatol* 126:2111–8

Jiveskog S, Ragnarsson-Olding B, Platz A, Ringborg U (1998) *N*-ras mutations are common in melanomas from sun-exposed skin of humans but rare in mucosal membranes or unexposed skin. *J Invest Dermatol* 111: 757–61

Kinzler KW, Vogelstein B (1997) Cancer-susceptibility genes. Gatekeepers and caretakers. *Nature* 386:761–3

Levy C, Khaled M, Fisher DE (2006) MITF: master regulator of melanocyte development and melanoma oncogene. *Trends Mol Med* 12:406–14

Lin JY, Fisher DE (2007) Melanocyte biology and skin pigmentation. *Nature* 445:843–50

Maitra A, Gazdar AF, Moore TO, Moore AY (2002) Loss of heterozygosity analysis of cutaneous melanoma and benign melanocytic nevi: laser capture microdissection demonstrates clonal genetic changes in acquired nevocellular nevi. *Hum Pathol* 33:191–7

Maldonado JL, Fridlyand J, Patel H, Jain AN, Busam K, Kageshita T *et al.* (2003) Determinants of BRAF mutations in primary melanomas. *J Natl Cancer Inst* 95:1878–90

Mancianti ML, Clark WH, Hayes FA, Herlyn M (1990) Malignant melanoma simulants arising in congenital melanocytic nevi do not show experimental evidence for a malignant phenotype. *Am J Pathol* 136:817–29

Molinaro AM, Simon R, Pfeiffer RM (2005) Prediction error estimation: a comparison of resampling methods. *Bioinformatics* 21:3301–7

Neckers L, Neckers K (2002) Heat-shock protein 90 inhibitors as novel cancer chemotherapeutic agents. *Expert Opin Emerg Drugs* 7:277–88

Ozisik YY, Meloni AM, Altungoz O, Peier A, Karakousis C, Leong SP *et al.* (1994) Cytogenetic findings in 21 malignant melanomas. *Cancer Genet Cytogenet* 77:69–73

Padilla RS, McConnell TS, Gribble JT, Smoot C (1988) Malignant melanoma arising in a giant congenital melanocytic nevus. A case report with cytogenetic and histopathologic analyses. *Cancer* 62:2589–94

Papp T, Pemsel H, Rollwitz I, Schipper H, Weiss DG, Schiffmann D *et al.* (2003) Mutational analysis of N-ras, p53, CDKN2A ($p16^{INK4a}$), $p14^{ARF}$, CDK4, and MC1R genes in human dysplastic melanocytic naevi. *J Med Genet* 40:E14

Papp T, Schipper H, Kumar K, Schiffmann D, Zimmermann R (2005) Mutational analysis of the BRAF gene in human congenital and dysplastic melanocytic naevi. *Melanoma Res* 15:401–7

Pavey S, Johansson P, Packer L, Taylor J, Stark M, Pollock PM *et al.* (2004) Microarray expression profiling in melanoma reveals a BRAF mutation signature. *Oncogene* 23:4060–7

Pollock PM, Harper UL, Hansen KS, Yudt LM, Stark M, Robbins CM *et al.* (2003) High frequency of BRAF mutations in nevi. *Nat Genet* 33: 19–20

Ray ME, Su YA, Meltzer PS, Trent JM (1996) Isolation and characterization of genes associated with chromosome-6 mediated tumor suppression in human malignant melanoma. *Oncogene* 12:2527–33

Rivers JK (2004) Is there more than one road to melanoma? *The Lancet* 363:728–30

Saaed AL, Sharov V, White J, Li J, Liang W, Bhagabati N *et al.* (2003) TM4: a free, open-source system for microarray data management and analysis. *Biotechniques* 34:374–8

Sharp S, Workman P (2006) Inhibitors of the HSP90 molecular chaperone: current status. *Adv Cancer Res* 95:323–48

Simon R, Radmacher MD, Dobbin K, McShane LM (2003) Pitfalls in the analysis of DNA microarray data: Class prediction methods. *J Natl Cancer Instit* 95:14–8

Stanton VP Jr, Cooper GM (1987) Activation of human raf transforming genes by deletion of normal amino-terminal coding sequences. *Mol Cell Biol* 7:1171–9

Tusher VG, Tibshirani R, Chu G (2001) Significance analysis of microarrays applied to the ionizing radiation response. *Proc Natl Acad Sci USA* 98:5116–21

Vance KW, Goding CR (2004) The transcription network regulating melanocyte development and melanoma. *Pigment Cell Res* 17: 318–325

Vandesompele J, De Preter K, Pattyn F, Poppe B, Van Roy N, De Paepe A *et al.* (2002) Accurate normalization of real-time quantitative RT-PCR data by geometric averaging of multiple internal control genes. *Genome Biol* 3: RESEARCH0034